Int. J. Heat Mass Transfer. Vol. 34, No. 10, pp. 2545–2553, 1991
Printed in Great Britain

0017-9310/91 $3.00+0.00

Assessment study of longitudinal rectangular plate inserts as tubeside heat transfer augmentative devices

JUN-DAR CHEN and SHOU-SHING HSIEH†
Department of Mechanical Engineering, National Sun Yat-Sen University, Kaohsiung, Taiwan 80424, Republic of China

(*Received* 1 *June* 1990 *and in final form* 26 *November* 1990)

Abstract—A number of longitudinal rectangular plate inserts used as tubeside heat transfer augmentative devices have been numerically investigated and assessed in the present study. The tube is of the axially uniform heat flux type with a peripherally constant wall temperature and an adiabatic rectangular plate insert. The flow is laminar, thermally developed and of steady state. The effects of the aspect ratio of the rectangular plate, the radius ratio of the circumscribed circle of the rectangular plate to the tube, and the eccentric installation on the net effect between heat transfer augmentation and pressure drop increase are determined.

INTRODUCTION

THE RECENT demand for high-efficiency heat transfer systems has stimulated interest in augmentative heat transfer methods in tubes. Meanwhile, to upgrade the energy utilization for existing systems, these methods are also appealing for the efficiency promotion of these systems, particularly where tubeside heat transfer coefficients are limiting due to the nature of the fluid. Designing a compact heat exchanger requires a high overall heat transfer coefficient and obviously enhancing tubeside heat transfer is one effective scheme toward this aim. In view of the above applications, enhanced heat transfer has truly become an attractive topic in both academic and industrial circles.

Whether external power is required or not, enhancement techniques can be classified as active and passive schemes. Each scheme includes various kinds of methods [1]. Among these methods, surface modifications [2, 3] or the use of inserts which are inserted into the flow channel to improve energy transport indirectly at the heated surface are of greatest interest for practical application. Due to their easy installations and cleaning operations, large numbers of potentially commercial inserts have been analysed in recent years. These include the twisted tapes [4, 5], wire coils [6], slat blockage [7], wire brush [8], flag-type insert [9], and spiral spring insert [10], just to name a few. Because the convective heat transfer coefficient is greatly increased by the centrifugal effect of swirl flow, inserts generating swirl flows are particularly attractive in applications. Nevertheless, as one may expect, an increase in the heat transfer coefficient will inevitably invoke the increase of pressure drop which is generally larger than the increase of heat transfer rate. On the other hand, even with lower heat transfer augmentation, the insert which does not generate swirl flow may also be an eligible augmentative device provided its net effect between the heat transfer augmentation and pressure drop increase is tolerable. Therefore, careful selection of the appropriate inserts must be made to optimize the heat transfer augmentation.

As one of the practical augmentative devices, a longitudinal rectangular plate is frequently inserted in the tubes of a tubular recuperator used for waste heat recovery. The cold combustion air flowing inside the tubes is heated by the hot waste gas which flows through the tube bundle. Figure 1 depicts the schematic diagram and relative geometric quantities of the flow passage of the cold combustion air. A series of works concerned with the laminar forced convection in a tube of axially uniform heat flux with peripherally uniform wall temperature and inserted with adiabatic plates of various aspect ratios had been performed by the authors. Relevant studies are extensively surveyed, and laminar forced convection of a plate insert with concentric and vertically eccentric installations are reported in ref. [11]. This paper presents, in addition to the laminar forced convection of a plate insert with horizontally eccentric installation, the assessment of the net effect between heat transfer augmentation and pressure drop increase of a plate insert. The effects of the aspect ratio of a plate insert, the radius ratio of the circumscribed circle of an insert to a tube, and the eccentric installation on the net effect of a plate insert are also determined.

THEORETICAL ANALYSIS

It is assumed that the thermophysical properties of the flowing fluid are constant, the flow is thermally

† Author to whom correspondence should be addressed.

NOMENCLATURE

A_f dimensionless flow area of passage (see equation (1))
A_f^* flow area of passage [m^2]
D_h dimensionless hydraulic diameter, d_h/R_o
d_h hydraulic diameter of the passage [m]
dp/dz axial pressure gradient [N m^{-3}]
EH, EV horizontal and vertical eccentricity ratios (see equation (1))
e_h, e_v horizontal and vertical eccentricities [m]
$f\,Re$ friction factor–Reynolds number product
H dimensionless height of the plate insert, h/R_o
h peripherally averaged heat transfer coefficient of the heated wall [W m^{-2} K^{-1}]; height of the plate insert [m]
J Jacobian of the transform
k thermal conductivity of fluid [W m^{-1} K^{-1}]
L dimensionless width of the plate insert, l/R_o
l width of the plate insert [m]
N dimensionless normal direction, n/R_o
Nu Nusselt number of the heated wall
n normal direction [m]
PL normalized peripheral location along the inner wall, $(\xi-\xi_{min})/(\xi_{max}-\xi_{min})$
P_o dimensionless perimeter of tube (see equation (1))
P_o^* perimeter of tube [m]
PR normalized pressure drop, $(-dp/dz)/(-dp/dz)_{bare}$
Q_p dimensionless overall heat transfer rate per unit pumping power (see equation (12))
QR normalized heat transfer rate, $h_m P_o^*/(h_m)_{bare} P_o^*$
q''_{in} axially uniform heat flux on tube [W m^{-2}]
R_o radius of tube [m]
RR radius ratio of the circumscribed circle of the insert to the tube, $0.5(L^2+H^2)^{0.5}$
T dimensionless temperature (see equation (1))
t temperature of fluid [K]
W dimensionless axial velocity (see equation (1))
w axial velocity [m s^{-1}]
X, Y dimensionless coordinates in the physical domain (see equation (1))
x, y coordinates in the physical domain [m].

Greek symbols

α, β, γ transformation coefficients
θ angular location (see Fig. 1) [deg]
μ dynamic viscosity of fluid [N s m^{-2}]
ξ, η dimensionless coordinates in the transformed domain
ρ density of fluid [kg m^{-3}]
τ overall wall shear stress [N m^{-2}].

Subscripts

b bulk value
bare value of bare tube
in inner wall
m mean value
s surface value at heated wall.

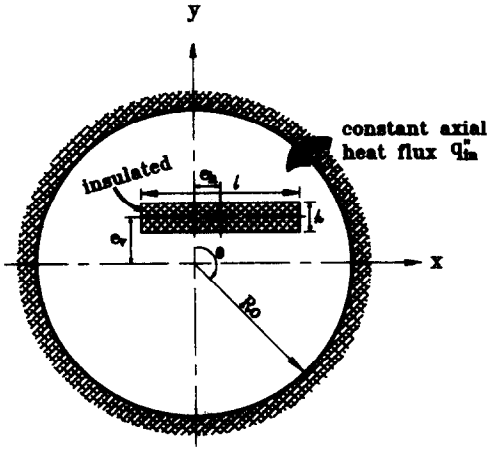

FIG. 1. Non-circular annular duct.

developed laminar and of steady state. The tube is assumed to be subject to an axially uniform heat flux and, due to its high conductive metallic material in practical application, peripherally uniform wall temperature t_s. The adiabatic condition is imposed on the plate insert to place the emphasis on the flow alternation by inserting such a plate and the consequent heat transfer alternation. In the analysis, the following dimensionless groups are employed:

$$X=\frac{x}{R_o};\quad Y=\frac{y}{R_o};\quad L=\frac{l}{R_o};\quad H=\frac{h}{R_o};\quad A_f=\frac{A_f^*}{R_o^2} \tag{1a}$$

$$P_o=\frac{P_o^*}{R_o};\quad W=\frac{w\mu}{(-dp/dz)R_o^2};\quad T=\frac{t-t_s}{q''_{in}R_o/k} \tag{1b}$$

$$EH = \frac{e_h/R_o}{1-RR}; \quad EV = \frac{e_v/R_o}{1-RR}. \tag{1c}$$

Under the above assumptions, the fluid temperature rising rate in the axial direction is related to q''_{in} via the overall heat balance and the dimensionless axial momentum and energy conservation equations are formulated as

$$\frac{\partial^2 W}{\partial X^2} + \frac{\partial^2 W}{\partial Y^2} + 1 = 0 \tag{2}$$

$$\frac{\partial^2 T}{\partial X^2} + \frac{\partial^2 T}{\partial Y^2} - \frac{WP_o}{W_m A_f} = 0. \tag{3}$$

The boundary conditions are mathematically expressed as

$$W = 0; \quad \frac{\partial T}{\partial N} = 0 \quad \text{at inner wall} \tag{4}$$

$$W = 0; \quad T = 0 \quad \text{at outer wall.} \tag{5}$$

The boundary-fitted coordinate system (BFCS) [12] is used to tackle the irregularity of the flow passage and equations (2) and (3) are transformed to this system as follows:

$$\frac{\partial}{\partial \xi}\left(\frac{\alpha}{J}\frac{\partial W}{\partial \xi} - \frac{\beta}{J}\frac{\partial W}{\partial \eta}\right) + \frac{\partial}{\partial \eta}\left(\frac{\gamma}{J}\frac{\partial W}{\partial \eta} - \frac{\beta}{J}\frac{\partial W}{\partial \xi}\right) + J = 0 \tag{6}$$

$$\frac{\partial}{\partial \xi}\left(\frac{\alpha}{J}\frac{\partial T}{\partial \xi} - \frac{\beta}{J}\frac{\partial T}{\partial \eta}\right) + \frac{\partial}{\partial \eta}\left(\frac{\gamma}{J}\frac{\partial T}{\partial \eta} - \frac{\beta}{J}\frac{\partial T}{\partial \xi}\right) - J\frac{WP_o}{W_m A_f} = 0 \tag{7}$$

where the transformation coefficients are defined as

$$J = X_\xi Y_\eta - X_\eta Y_\xi; \quad \alpha = X_\eta^2 + Y_\eta^2 \tag{8a}$$

$$\gamma = X_\xi^2 + Y_\xi^2; \quad \beta = X_\xi X_\eta + Y_\xi Y_\eta. \tag{8b}$$

By the generation method with elliptic differential equations [12], a 73×36 non-orthogonal boundary-fitted grid in the physical domain is numerically generated with nodes equi-spaced along, and more grid lines closely packed near both walls. The governing equations, equations (6) and (7), with boundary conditions, equations (4) and (5), are solved by the finite-volume discretized method with SLOR solver in the transformed domain and the over-relaxation factor for each variable is chosen as 1.7. In each run, the iteration procedure is terminated when the absolute deviation (relative to the variable value of the present iteration) between two consecutive iterations is less than 10^{-5} for each variable at each node. The $f\,Re$ factor and the local and averaged outer wall Nusselt numbers are defined as follows:

$$f\,Re = [\tau/(\rho w_m^2/2)](\rho w_m d_h/\mu) = D_h^2/(2W_m) \tag{9}$$

$$Nu = -\left(\frac{\partial t}{\partial n}\right)_s d_h/(t_s - t_b) = \left(\frac{\partial T}{\partial N}\right)_s D_h/T_b \tag{10}$$

and

$$Nu_m = q''_{in} d_h/[k(t_s - t_b)] = -D_h/T_b. \tag{11}$$

Although several criteria for evaluating the performance of the enhancing technique are proposed in the literature [13, 14], that suggested by Lau *et al.* [15] is more convenient to use in numerical study and is thereby adopted in this work. As a criterion for evaluating the net effect of an insert, the dimensionless overall heat transfer rate per unit pumping power, Q_p, is defined as [15]

$$Q_p = QR/PR^{1/3} \tag{12}$$

where QR and PR denote the normalized heat transfer rate and pressure drop, respectively, with their corresponding bare tube values for the same mass flow rate. A value of Q_p greater than or equal to unity denotes a positive effect, but others denote a negative, net effect. By the definition and $(f\,Re)_{bare} = 16$, $(Nu_m)_{bare} = 4.36$ and $(d_h)_{bare} = 2R_o$, PR and QR are expressed as

$$PR = \frac{f\,Re}{(f\,Re)_{bare}} \frac{(d_h)_{bare}^2}{d_h^2} \frac{w_m}{(w_m)_{bare}} = \frac{f\,Re}{4D_h^2} \frac{\pi}{A_f} \tag{13}$$

$$QR = \frac{q''_{in}/(t_s - t_b)}{(Nu_m)_{bare} k/(d_h)_{bare}} = -0.4587/T_b. \tag{14}$$

RESULTS AND DISCUSSION

Laminar forced convection in some annular passages where results are available [16, 17] is examined to test the accuracy of the present solution procedure. Laminar forced convection in a tube with a concentric square inner core solved by Solanki *et al.* [16] is run. Figure 2 compares the calculated values of Nu_m with those in ref. [16]. Also compared in Fig. 2 are the calculated $f\,Re$ factors with those documented by Shah and London [17]. For laminar forced convections in concentric/eccentric circular annuli with thermal boundary condition of one wall with Dirichlet, and the other with Neumann, condition, Fig. 3 compares the RR dependencies of the $f\,Re$ factor and the Nu_m value obtained by the present procedure and those documented by Shah and London [17]. Agreements in the above comparisons are found to be good with a maximum deviation of the order of 1%. According to the aforementioned evaluating criterion,

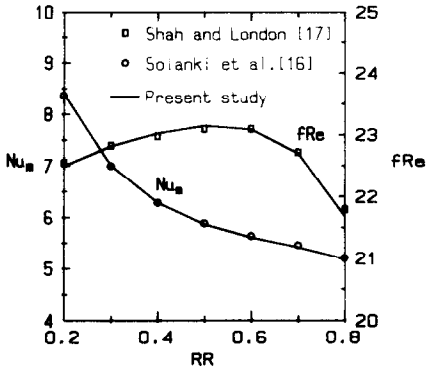

FIG. 2. Comparison of Nu_m value and $f\,Re$ factor in a concentric, non-circular annulus.

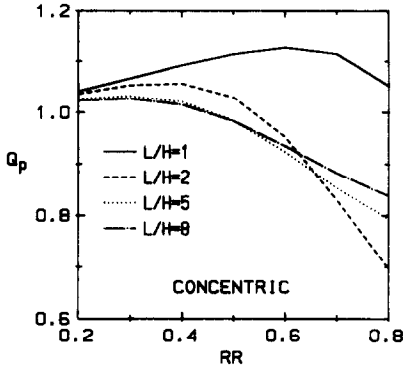

FIG. 4. RR dependencies of Q_p value of various inserts in a concentric installation.

net effect assessments for plate inserts are made in sequence for concentric and eccentric installations.

Concentric installation case

Laminar forced convection in a tube with concentric plate inserts of aspect ratio (L/H) of 1, 2, 5 and 8 had been reported in ref. [11], thus only the net effect assessments of these inserts are provided here.

Table 1. Concentric installation case

L/H	RR	PR	QR	Q_p
1	0.200	2.116	1.338	1.042
	0.500	5.118	1.920	1.114
	0.800	19.272	2.821	1.052
2	0.200	2.042	1.315	1.037
	0.500	4.278	1.671	1.029
	0.800	9.969	1.501	0.697
5	0.200	1.885	1.268	1.027
	0.500	3.087	1.434	0.985
	0.800	4.409	1.302	0.794
8	0.200	1.829	1.252	1.023
	0.500	2.789	1.384	0.983
	0.800	3.598	1.285	0.838

Table 1 summarizes the PR, QR and Q_p values of these inserts for various RR values and the dependencies of their Q_p values on the RR value are plotted in Fig. 4. For all RR values, both PR and QR values are larger than unity which implies that concentrically inserting the plate indeed augments heat transfer but inevitably invokes the pressure drop increase. Because of the increase of the blockage effect of the insert, increasing the RR value causes the PR values of all inserts to increase. For the same RR value, comparing the PR values of all inserts reveals that the blockage effect becomes more evident and, consequently, results in the increase of QR value as the L/H value decreases.

For the insert of $L/H = 1$ (square), the QR value increases more slowly than the PR value with increasing RR value and, eventually, the Q_p value increases first then reaches a maximum at a certain RR value (Fig. 4). For any other studied plate insert, the PR value increases with the RR value but the QR value reaches a maximum at a certain RR value. Figure 4 indicates that, for plate inserts of $L/H \geqslant 2$, the Q_p values decrease monotonically with increasing RR value as $RR \geqslant \approx 0.4$. The larger the aspect ratio, the slower the decreasing rate of the Q_p value. As a result, among these inserts, while the insert of $L/H = 2$ has

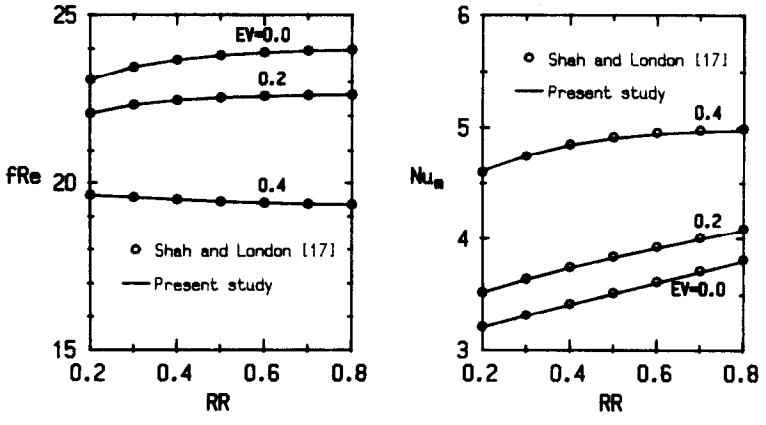

FIG. 3. Comparison of Nu_m value and $f\,Re$ factor in a concentric and eccentric circular annulus.

the highest Q_p value as $RR \leqslant \approx 0.63$, the Q_p value of the insert of $L/H = 8$ becomes the largest for larger RR values. While the square insert has a positive net effect for all studied RR values, each plate insert has a positive net effect only when the RR value is less than its own critical RR value. Note that the plate insert of higher aspect ratio has a lower critical RR value. Generally speaking, the square insert has a higher net effect than any other studied plate insert for each RR value.

Eccentric installation case

Only two typical inserts of $L/H = 1$ (square) and 5 (thin plate) are considered for the horizontally eccentric installation case with EH value ranging from 0.0 to 0.4. The distributions of isotherms and isovels of axial velocity (normalized with respect to W_m) of both inserts with horizontally eccentric installations are shown in Fig. 5. Due to the symmetric nature, isotherms are plotted in the upper half and isovels in the lower half with the dot denoting the position of the $(W/W_m)_{max}$ value. The contour values are equi-spaced with the spacing listed below the figure. Also listed are the T_{min} and $(W/W_m)_{max}$ values. As can be seen from Fig. 5, the radial distribution of the W/W_m value at each angular location is almost parabolic with a peak somewhat close to the inner wall. Fluid temperatures are negative because of the definition of dimensionless temperature and the thermal boundary condition employed.

Due to the shrinkage in the right gap, and enlargement in the left gap, of the clearance, rightward shifting the insert decreases the flow rate through the right gap and increases that through the left gap. As a result, the isotherms are clockwise twisted and fluid temperature becomes more angularly variant. Fluid temperature in the right gap becomes higher and more uniform than in other regions. For the square insert with horizontally eccentric installation, the highest W/W_m peak occurs at the angular location through the midpoint of the left-hand side of the insert (same as in the concentric case [11]). However, the angular location with the lowest W/W_m peak shifts from that through the corners in concentric cases [11] toward the right gap in accordance with the decrease of the flow rate there. It is noticed that rightward shifting of the thin plate insert shifts the angular location of the largest W/W_m value to the left.

Distributions of both wall temperatures are also of practical interest. Due to the assumption of uniform outer wall temperature, only peripheral variations of inner wall temperature, T_{in}, are provided and depicted in Figs. 6 and 7 for the square insert and the thin plate insert, respectively, of $RR = 0.5$. The peripheral location, PL, is measured from the midpoint of the upper side of the insert. For the square insert, the

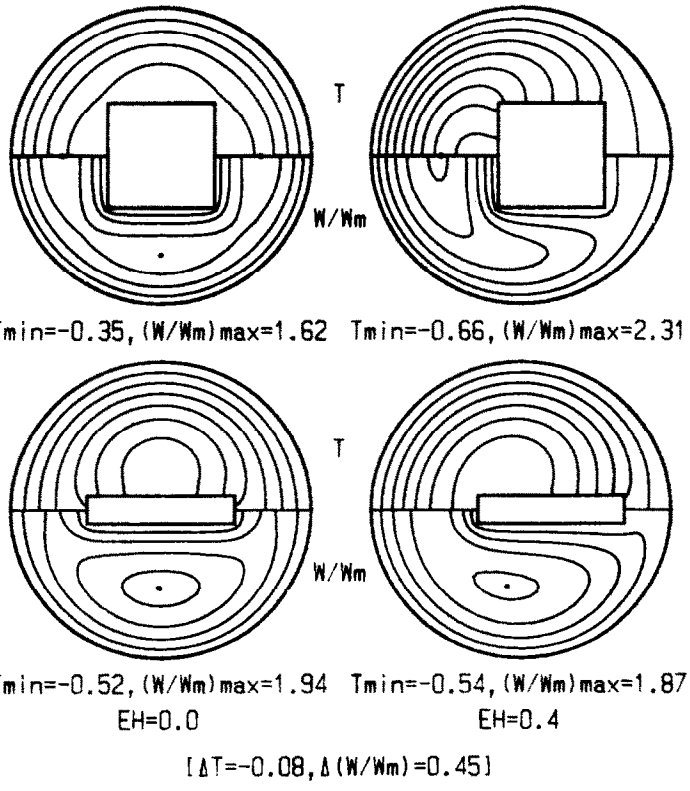

FIG. 5. Flow and temperature patterns for horizontally eccentric installations of inserts.

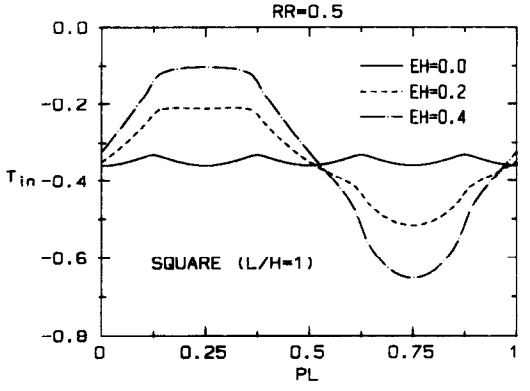

FIG. 6. Variation of T_{in} along the peripheral direction of a square insert in a horizontally eccentric installation.

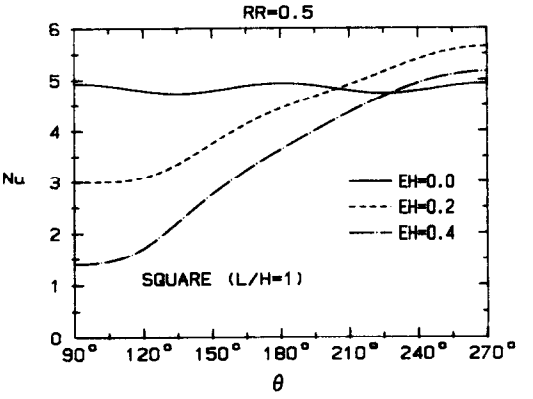

FIG. 8. Angular variation of Nu value in a tube with a horizontally eccentric square insert.

wavy variation of T_{in} in the concentric case changes to variation of sine-like shape due to the redistribution of the cross-sectional flow rate. The largest and lowest T_{in} values increase and decrease, respectively, with the increase of the EH value. The T_{in} values in the right gap ($0.125 \leqslant PL \leqslant 0.375$) are nearly uniform in the horizontally eccentric case. As for the thin plate insert, the variation type of the T_{in} value is unchanged in the studied range of EH value. Nevertheless, the T_{in} value at $PL = 0.25$ (midpoint of the insert side in the right gap) increases and that at $PL = 0.75$ (midpoint of the insert side in the left gap) decreases. Moreover, the PL value where the lowest T_{in} value occurs increases with the increases of EH value, which can be attributed to the leftward shift of the largest W/W_m value. As the EH value increases, the T_{in} value becomes more peripherally non-uniform.

Figures 8 and 9 display the angular variations of Nu values of the square insert and thin plate insert, respectively, of $RR = 0.5$ with horizontally eccentric installation. The θ angle in these figures is measured clockwise from the positive Y-axis (Fig. 1). Due to the symmetric nature of the flow and temperature patterns, such variations are presented over θ values ranging from 90° (through the centre of the right gap) to 270° (through the centre of the left gap). For each insert, rightward shifting significantly reduces the Nu values in the right gap and causes those in the left gap to approach uniform distribution. Figure 8 reveals that, when the square insert is shifted to the right, the largest Nu value occurs at $\theta = 270°$ and the difference between the largest and lowest Nu values increases with the increase of EH value. In accordance with the alternation of isotherm distribution, rightward shifting the thin plate insert increases the θ value where the largest Nu value appears and decreases the largest Nu value, as depicted in Fig. 9. To supplement information for design, Table 2 summarizes the Nu_m value and the $f\,Re$ factor of square and thin plate inserts with horizontally eccentric installation. For the square insert, both the Nu_m value and the $f\,Re$ factor decrease with the increase of EH value for each RR value. However, it is not always the case for the thin plate insert. The exception occurs as $RR > \approx 0.6$ where the Nu_m value increases with increasing EH value.

The influences of both horizontally and vertically eccentric installations on the net effect of the insert are investigated over EH and EV values ranging from 0.0 to 0.4. Tables 3 and 4 summarize the PR, QR and Q_p values of the square insert and the thin plate insert,

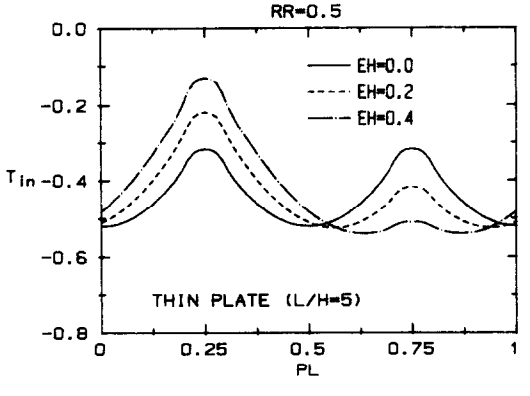

FIG. 7. Variation of T_{in} along the peripheral direction of a thin plate insert in a horizontally eccentric installation.

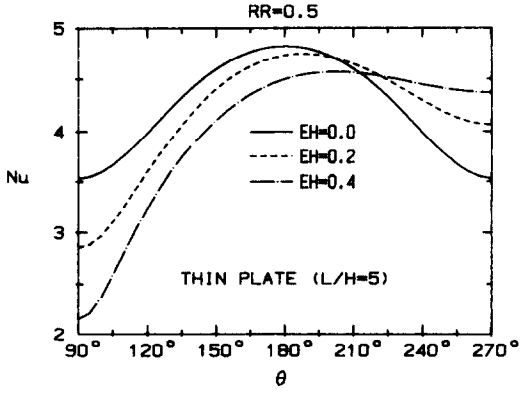

FIG. 9. Angular variation of Nu value in a tube with a horizontally eccentric thin plate insert.

Table 2. Overall $f\,Re$ factors and Nu_m values for horizontally eccentric installations of various inserts

EH	RR	Square ($L/H = 1$) $f\,Re$	Square ($L/H = 1$) Nu_m	Thin plate ($L/H = 5$) $f\,Re$	Thin plate ($L/H = 5$) Nu_m
0.0	0.2	22.50	4.818	22.15	4.762
	0.4	23.03	4.852	22.23	4.552
	0.6	23.09	4.806	20.46	3.863
	0.8	21.68	4.237	16.54	2.993
0.2	0.2	21.65	4.494	21.47	4.557
	0.4	22.12	4.362	21.69	4.411
	0.6	22.33	4.308	20.24	3.852
	0.8	21.33	4.003	16.51	3.000
0.4	0.2	19.50	3.923	19.72	4.153
	0.4	19.80	3.546	20.26	4.089
	0.6	20.35	3.427	19.60	3.815
	0.8	20.34	3.468	16.43	3.018

Table 3. Eccentric installation of square insert ($L/H = 1$)

EV/EH	RR	PR	QR	Q_p
0.0	0.200	2.116	1.338	1.042
	0.500	5.118	1.920	1.114
	0.800	19.272	2.821	1.052
0.2	0.200	2.036	1.248	0.985
	0.500	4.926	1.713	1.007
	0.800	18.961	2.665	1.000
0.4	0.200	1.834	1.090	0.890
	0.500	4.435	1.366	0.831
	0.800	18.081	2.310	0.880

Table 4. Eccentric installation of thin plate insert ($L/H = 5$)

EV	EH	RR	PR	QR	Q_p
0.4	0.0	0.200	1.660	1.058	0.893
		0.500	2.775	1.102	0.784
		0.800	4.292	1.198	0.737
0.2	0.0	0.200	1.822	1.194	0.977
		0.500	3.002	1.317	0.913
		0.800	4.380	1.273	0.778
0.0	0.0	0.200	1.885	1.268	1.027
		0.500	3.087	1.434	0.985
		0.800	4.409	1.302	0.794
0.0	0.2	0.200	1.827	1.214	0.993
		0.500	3.032	1.411	0.975
		0.800	4.401	1.305	0.796
0.0	0.4	0.200	1.678	1.106	0.931
		0.500	2.882	1.352	0.950
		0.800	4.380	1.313	0.802

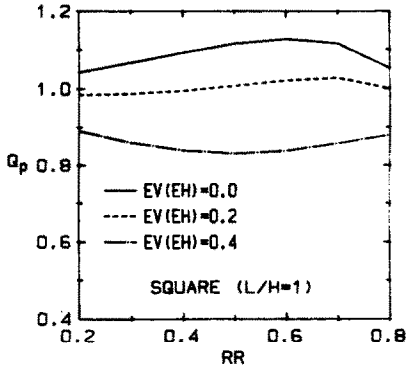

FIG. 10. Effect of RR value for the eccentric installation of a square insert.

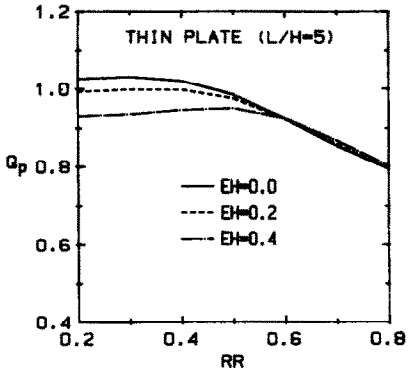

FIG. 11. Effect of RR value for the horizontally eccentric installation of a thin plate insert.

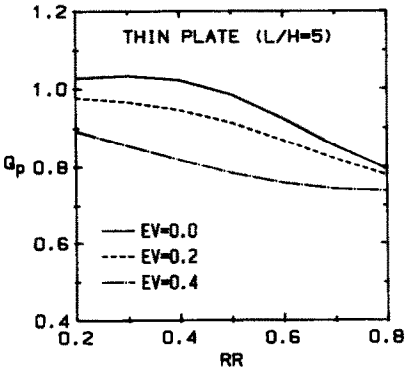

FIG. 12. Effect of RR value for the vertically eccentric installation of a thin plate insert.

respectively, with both eccentric installations. The RR dependencies of Q_p values of the square insert with both eccentric installations are plotted together in Fig. 10 due to their equivalence in laminar forced convection. The equivalence is not valid for the thin plate insert and such dependencies of horizontally and vertically eccentric cases are separately plotted in Figs. 11 and 12. Note that PR and QR values are also larger than unity in both eccentric installations.

For each RR value, Table 3 indicates that increasing the eccentricity ratio decreases the PR, QR and Q_p values of the square insert simultaneously and, as shown in Fig. 10, the RR dependence of the Q_p value varies with the EH value. With both eccentric installations, the square insert is eligible as a tubeside augmentative device as long as the eccentricity ratio is

lower than about 0.2. Figure 11 indicates that eccentrically installing the thin plate insert horizontally will decrease the Q_p value when $RR \leqslant \approx 0.6$, but only increases Q_p slightly when $RR > \approx 0.6$. For any given RR value, the Q_p value of the thin plate insert is decreased in the vertically eccentric installation case and the decrease in Q_p value is largest near $RR = 0.5$, as evidenced in Fig. 12. Generally speaking, eccentric installation makes the thin plate insert ineligible as an augmentative device except for such an insert of small RR value with small eccentricity ratio. With the same incremental change in eccentricity ratio, Figs. 10–12 also show that, for each RR value, the larger the eccentricity ratio, the larger the change in Q_p value. A close examination of Table 4 reveals that, under the same value of eccentricity ratio, the thin plate insert with horizontally eccentric installation has a higher net effect than with vertically eccentric installation.

Figure 13 compares the influence of the aspect ratio of the plate insert on its Q_p value for plate inserts of $RR = 0.5$ with vertically eccentric installation. In addition to inserts of $L/H = 1$ and 5, two inserts of $L/H = 2$ and 8 are also included for comparison. With the increase of EV value, the Q_p value of each insert decreases gradually at small EV value but more rapidly at larger EV values. The larger the aspect ratio of the plate insert, the lower the decreasing rate of the Q_p value. Although not shown explicitly, this is also the case for plate inserts with horizontally eccentric installation as evidenced in Figs. 10 and 11. From these trends, it can therefore be inferred that eccentric installation will decrease the aforementioned critical RR value of the plate insert of $L/H \geqslant 2$ in the concentric case.

Since the square insert has the best net effect in the concentric case for each RR value, it is interesting to investigate whether it is also true in the eccentric cases. Comparing both Tables 3 and 4 reveals that, with horizontally eccentric installation, the thin plate insert has a better net effect than the square insert when the RR value is smaller than a certain RR value which increases with the increase of EH value. This implies that, with horizontally eccentric installation, the square insert will lose its superiority as an augmentative device to a thin plate insert at some RR values. With vertically eccentric installation, the square insert is found having better net effect than the thin plate insert except for the case of $RR = 0.2$ and $EV = 0.4$. However, the discrepancy between Q_p values of both inserts in this special case is too small to distinguish and can therefore be neglected. Roughly speaking, vertically eccentric installation can be claimed to have no influence on the superiority of the square insert to the thin plate insert.

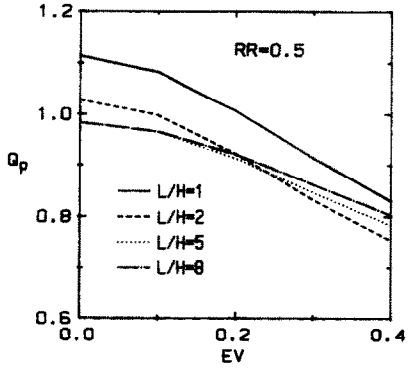

FIG. 13. Effect of EV value for various inserts.

CONCLUSION

An assessment study for a number of rectangular plate inserts as tubeside heat transfer augmentative devices has been performed. Both concentric and eccentric installations of these inserts are taken into account. Also provided are the heat transfer and fluid friction characteristics for horizontally eccentric installation of some inserts. Based on the results of the present study, the following conclusions can be drawn:

(1) In the case of concentric installation, the square insert has a higher net effect than any other plate insert and can be used as a tubeside augmentative device for all RR values studied. However, each plate insert of $L/H \geqslant 2$ becomes eligible only when the RR value is less than its own critical RR value. The larger the aspect ratio of the plate insert, the smaller its critical RR value.

(2) For a plate insert with a horizontally eccentric installation, the flow rate through a gap formed by the insert and the tube is proportional, but fluid and inner wall temperatures there are inversely proportional, to the gap clearance. For each RR value, horizontally eccentric installation of studied plate inserts decreases their $f\,Re$ factors. The Nu_m values of these inserts are also decreased by this geometric alternation except for the thin plate insert of $RR > \approx 0.6$.

(3) Eccentric installation of the square insert degrades the net effect for each RR value. While this is also true for the thin plate insert with vertically eccentric installation, horizontally eccentric installation of this insert shows a similar trend when $RR \leqslant \approx 0.6$ but is opposite when $RR > \approx 0.6$. Under the same incremental change in eccentricity ratio, the larger the eccentricity ratio, the larger the change in Q_p value of each insert.

(4) Despite horizontally or vertically eccentric installation, the square insert of any RR value studied can be used to enhance tubeside heat transfer as long as the eccentricity ratio is small. The critical RR value over which the thin plate insert becomes ineligible varies with eccentric type and eccentricity ratio. A thin plate insert with a horizontally eccentric installation has a higher net effect than with a vertically eccentric installation.

(5) The superiority of a square insert to a thin plate insert as an augmentative device in the concentric case will not be influenced by the vertically eccentric installation. However, a horizontally eccentric installation causes the square insert to lose its superiority to the thin plate insert over an *RR* range which increases with the increase of *EH* value.

REFERENCES

1. A. E. Bergles, Some perspectives on enhanced heat transfer—second generation heat transfer technology, *J. Heat Transfer* **110,** 1082–1096 (1988).
2. B. W. Webb and S. Ramadhyani, Conjugate heat transfer in a channel with staggered ribs, *Int. J. Heat Mass Transfer* **28,** 1679–1687 (1985).
3. I. M. Rustum and H. M. Soliman, Numerical analysis of laminar forced convection in the entrance region of tubes with longitudinal internal fins, *J. Heat Transfer* **110,** 310–313 (1988).
4. S. W. Hong and A. E. Bergles, Augmentation of laminar flow heat transfer in tubes by means of twisted-tape inserts, *J. Heat Transfer* **98,** 251–256 (1976).
5. J. P. Du Plessis and D. G. Hroger, Heat transfer correlation for thermally developing laminar flow in a smooth tube with a twisted-tape insert, *Int. J. Heat Mass Transfer* **30,** 509–515 (1987).
6. S. B. Uttarwar and M. R. Rao, Augmentation of laminar flow heat transfer in tubes by means of wire coil inserts, *J. Heat Transfer* **107,** 930–935 (1985).
7. E. M. Sparrow, K. K. Koran and M. Charmichi, Heat transfer and pressure drop characteristics induced by a slat blockage in a circular tube, *J. Heat Transfer* **102,** 64–70 (1980).
8. F. F. Megerlin, R. W. Murphy and A. E. Bergles, Augmentation of heat transfer in tubes by use of mesh and brush inserts, *J. Heat Transfer* **96,** 145–151 (1974).
9. J. L. Fernandez and R. Poulter, Heat transfer enhancement by means of flag-type insert in tubes, *Int. J. Heat Mass Transfer* **30,** 2603–2609 (1987).
10. J. P. Chiou, Experimental investigation of the augmentation of forced convection heat transfer in a circular tube using spiral spring inserts, *J. Heat Transfer* **109,** 300–307 (1987).
11. J. D. Chen and S. S. Heish, Laminar forced convection in circular duct inserted with a longitudinal rectangular plate, *J. Thermophys. Heat Transfer* (to appear).
12. J. F. Thompson, F. C. Thames and C. W. Mastin, TOMCAT—a code for numerical generation of boundary fitted curvilinear coordinate systems of fields containing any number of arbitrary 2-D bodies, *J. Comput. Phys.* **24,** 274–302 (1977).
13. A. E. Bergles, A. R. Blumenkrantz and J. Taborek, Performance evaluation criteria for enhanced heat transfer surfaces, *Proc. Int. Heat and Mass Transfer Conf.*, Vol. 2, pp. 239–243 (1974).
14. R. L. Webb, Performance evaluation criteria for use of enhanced heat transfer surfaces in heat exchanger design, *Int. J. Heat Mass Transfer* **24,** 715–726 (1981).
15. S. S. Lau, L. E. Ong and J. C. Han, Conjugate heat transfer in channels with internal longitudinal fins, *J. Thermophys. Heat Transfer* **3,** 303–308 (1989).
16. S. C. Solanki, S. Prakash, J. S. Saini and C. P. Gupta, Forced convection heat transfer in doubly connected ducts, *Int. J. Heat Fluid Flow* **8,** 107–110 (1987).
17. R. K. Shah and A. L. London, *Laminar Flow Forced Convection in Ducts*, pp. 284–353. Academic Press, New York (1978).

EVALUATION D'INSERTS PLANS RECTANGULAIRES DU POINT DE VUE DE L'AUGMENTATION DU TRANSFERT THERMIQUE POUR UN TUBE

Résumé—On considère et évalue numériquement l'avantage d'inserts plans rectangulaires longitudinaux utilisés pour augmenter le transfert thermique à la surface d'un tube. Ce tube est chauffé à flux uniforme axialement avec une température constante sur la périphérie et insert rectangulaire plan adiabatique. L'écoulement est laminaire thermiquement établi et permanent. On détermine les effets d'augmentation de transfert thermique et de perte de charge des paramètres comme le rapport de forme des plaques rectangulaires, le rapport du rayon du cercle circonscrit aux plaques à celui du tube et l'installation avec excentricité.

ABSCHÄTZUNG DER VERBESSERUNG DES WÄRMEÜBERGANGS IN EINEM ROHR DURCH DEN EINBAU RECHTECKIGER EBENER STREIFEN IN LÄNGSRICHTUNG

Zusammenfassung—In der vorliegenden Arbeit wird der Einfluß unterschiedlicher steifenartiger Einbauten auf den Wärmeübergang in einem Rohr numerisch untersucht und abgeschätzt. Das Rohr wird in axialer Richtung gleichförmig beheizt, wobei die Wandtemperatur am Unfang konstant und die eingebauten Streifen adiabat sind. Die Strömung ist laminar, thermisch ausgebildet und stationär. Der Einfluß folgender Größen auf die Verbesserung des Wärmeübergangs und die Erhöhung des Druckabfalls werden bestimmt: Seitenverhältnis des Streifens, Verhältnis zwischen dem Radius des den Rechteckstreifen umschreibenden Kreises und dem Rohrradius sowie Exzentrizität des Einbaus.

ОЦЕНКА ВЛИЯНИЯ ПРОДОЛЬНЫХ ПРЯМОУГОЛЬНЫХ ПЛАСТИНЧАТЫХ ВСТАВОК, ИСПОЛЬЗУЕМЫХ В КАЧЕСТВЕ УСИЛИТЕЛЕЙ ТЕПЛОПЕРЕНОСА В ТРУБАХ

Аннотация—Численно исследуется и оценивается влияние ряда продольных прямоугольных вставок, используемых в качестве усилителей теплопереноса в трубах. Труба со вставленной в нее адиабатической прямоугольной пластиной находится в условиях аксиального однородного теплового потока и имеет постоянную по окружности температуру стенки. Течение является ламинарным, термически развитым и стационарным. Определяется влияние отношения сторон прямоугольной пластины, отношения радиуса круга, описываемого прямоугольной пластиной, к радиусу трубы, а также эксцентриситета на взаимосвязь между интенсификацией теплопереноса и увеличением перепада давления.